Driving Neuromodules into Synchronous Chaos *

Frank Pasemann
Max-Planck-Institute for Mathematics in the Sciences
Inselstr. 22–26, D-04103 Leipzig, Germany
email: f.pasemann@mis.mpg.de

Abstract

We discuss the time-discrete parametrized dynamics of two neuromodules, which are coupled in a uni-directional way. General conditions for the existence of synchronized dynamics are derived for these systems. It is demonstrated that already the one-way couplings of 2-neuron modules can result in periodic, quasiperiodic as well as chaotic dynamics constrained to a synchronization manifold M. Stability of the synchronized dynamics is calculated by conditional Lyapunov exponents. In addition to synchronized attractors there often co-exist asynchronous periodic, quasiperiodic or even chaotic attractors. Simulation results for selected sets of parameters are presented.

*partly in: Mira, J., and Sanchez-Andres (eds.), *Foundations and Tools for Neural Modeling*, IWANN'99, Alicate, Spain, June 1999, Proceedings, Vol. I, LNCS **1606**, Springer, Berlin, pp. 377–384.

1 Introduction

In a paper by Pecora and Carroll [7] it was established for the first time that synchronization of chaotic systems is possible. Since then, many articles investigated this phenomenon, often because of its importance for applications in the field of secure communication. (cf. e.g. citations in [2]). Most of the work analyses the dynamics of coupled time-continuous systems, like Chua's circuit, or Lorenz or Rössler systems. But also time-discrete systems have been studied [3].

On the other hand, selective synchronization of neural activity in biological brains was often suggested to be a fundamental temporal mechanism for binding spatially distributed features into a coherent object (cf. e.g. [9]). Thus, studying the properties of synchronized dynamics in coupled chaotic neuromodules may not only induce new explanatory models for cognitive functions of biological brains, but may also provide interesting models for the generation of higher level information processes in artificial neural systems. Typically, coupled neuromodules are endowed with a large set of parameters (synaptic weights and bias terms/stationary inputs), which allow not only synchronization but also a fast de-synchronization of module dynamics.

The term "synchronization" will be used here in the sense of *complete synchronization*; i.e. we consider systems, the states of which can coincide, while the dynamics in time remains, for instance, chaotic. We also discern between global and local synchronization. Global synchronization means that for almost all initial conditions the orbits of the systems will synchronize. Local synchronization refers to stable synchronized states; i.e. small perturbations will not de-synchronize the systems.

In this contribution we study the synchronized discrete dynamics of two neuromodules, which are assembled to a composed system through a one-way coupling. The modules have the same number of additive graded neurons. In section 2 we derive general conditions for the existence of synchronized dynamics of the coupled modules and for the stability of synchronized states. Results of computer simulations are presented for a specific example in section 3. It uses a chaotic 2-neuron module with self-inhibiting neuron coupled bi-directionally to an excitatory neuron [4]. The driven system is a 2-neuron module oscillating with period-4. This setup has larger parameter domains for which global as well as local synchronization of periodic, quasiperiodic and chaotic dynamics is observed. Synchronized orbits are not always stable; this can be read from the *conditional* Lyapunov exponents first introduced in [7]. The boundary between stable and unstable synchronization of chaos corresponds to switching from a chaotic to a hyperchaotic [8] regime of the coupled system. Furthermore, computer simulations demonstrate that various asynchronous attractors may co-exist with attractors constrained to the manifold M of synchronized states.

2 Coupled neuromodules

We are considering a neuromodule with n units as a discrete parametrized dynamical system on an n-dimensional activity phase space $\mathbf{R}^n$. With respect to a set ρ of parameters it is given by the map $f_\rho : \mathbf{R}^n \to \mathbf{R}^n$ defined by

$$a_i(t+1) = \theta_i + \sum_{j=1}^{n} w_{ij}\, \sigma(a_j(t)) \;, \quad i = 1, \ldots, n \;, \tag{1}$$

where $a_i \in \mathbf{R}^n$ denotes the activity of the i-th neuron, and $\theta_i = \overline{\theta}_i + I_i$ denotes the sum of its fixed bias term $\overline{\theta}_i$ and its stationary external input I_i. The output $o_i = \sigma(a_i)$ of a unit is given by the standard sigmoidal transfer function $\sigma(x) := (1 + e^{-x})^{-1}$, $x \in \mathbf{R}$, and w_{ij} denotes the synaptic weight from unit j to unit i. If there exists a parameter set $\rho = (\theta, w)$ for which the dynamics (1) has at least one chaotic attractor, the module will be called a *chaotic neuromodule*.

Now, let A and B denote two neuromodules (1) with parameter sets $\rho^A = (\theta^A, w^A)$ and $\rho^B = (\theta^B, w^B)$, respectively. The neural activities of module A and B will be denoted a_i, b_i, $i = 1, \ldots, n$, respectively. Connections going from module B to module A are given by $(n \times n)$-coupling matrix w^{AB}. Correspondingly, connections from module A to module B are given as a matrix w^{BA}. Thus, the architecture of the $2n$-dimensional coupled system is given by a matrix w of the form

$$w = \begin{pmatrix} w^A & w^{AB} \\ w^{BA} & w^B \end{pmatrix} . \tag{2}$$

In the following we will consider the process of *complete synchronization*, i.e. there exists a subset $D \subset \mathbf{R}^{2n}$ such that $(a_0, b_0) \in D$ implies

$$\lim_{t \to \infty} \mid a(t; a_0) - b(t; b_0) \mid = 0 \;,$$

where $(a(t; a_0), b(t; b_0))$ denotes the orbit under F_ρ through the initial condition $(a_0, b_0) \in \mathbf{R}^{2n}$. Thus we are interested in the case where corresponding neurons of the modules have identical activities during a process. The synchronization is called *global* if $D \equiv \mathbf{R}^{2n}$, and *local* if $D \subset \mathbf{R}^{2n}$ is a proper subset. Thus, a *synchronized state* s of the coupled system is defined by $s := a = b \in \mathbf{R}^n$. The *synchronization manifold* $M := \{(s, s) \in \mathbf{R}^{2n} \mid s = a = b\}$ of synchronized states corresponds to an n-dimensional hyperplane $M \cong \mathbf{R}^n \subset \mathbf{R}^{2n}$.

A straight forward calculation will prove the following general synchronization condition:

Lemma 1 *Let the parameter sets ρ^A, ρ^B of the modules A and B satisfy*

$$\theta := \theta^A = \theta^B \;, \quad (w^A - w^{BA}) = (w^B - w^{AB}) \;. \tag{3}$$

Then every orbit of F_ρ through a synchronized state $s \in M$ is constrained to M for all times.

Here we will be interested in the special case of uni-directional couplings between modules; i.e., with $w^{AB} = 0$, module B is driven by the dynamics of module A. The general synchronization condition (3) then reduces to

$$\theta := \theta^A = \theta^B \ , \quad (w^A - w^{BA}) = w^B \ . \tag{4}$$

Using this last condition (4), and introducing new coordinates parallel and orthogonal to the synchronization manifold M by

$$\xi_i := \frac{1}{\sqrt{2}}(a_i + b_i) \quad , \quad \eta_i := \frac{1}{\sqrt{2}}(a_i - b_i) \ , \quad i = 1, \ldots, n \ , \tag{5}$$

the dynamics $\tilde{F}_\rho$ of two uni-directionally coupled n-modules is given by

$$\begin{aligned} \xi_i(t+1) &= \sqrt{2} \cdot \theta_i + \frac{1}{\sqrt{2}} \sum_{j=1}^{n} [w_{ij}^{+} \cdot g^{+}(\xi_j(t), \eta_j(t)) + w_{ij}^{B} \cdot g^{-}(\xi_j(t), \eta_j(t))] \ , \\ \eta_i(t+1) &= \frac{1}{\sqrt{2}} \sum_{j=1}^{n} w_{ij}^{B} \cdot (g^{+}(\xi_j(t), \eta_j(t)) - g^{-}(\xi_j(t), \eta_j(t))) \ , \end{aligned} \tag{6}$$

where $i = 1, \ldots, n$, and we have set $w^{+} := (w^A + w^{BA})$; the functions $g^{\pm}$ are defined by

$$g^{\pm}(x, y) := \sigma\left(\frac{1}{\sqrt{2}}\,(x \pm y)\right) \ , \quad x,\ y \in \mathbf{R} \ .$$

Setting $\eta = 0$ and $s = 1/\sqrt{2}\,\xi$, the synchronized n-dimensional dynamics F_ρ^s constrained to the manifold M is derived from equations (6). It reads

$$s_i(t+1) = \theta_i + \sum_{j=1}^{n} w_{ij}^{A} \cdot \sigma(s_j(t)) \ , \tag{7}$$

i.e., because of the uni-directional coupling, the synchronized dynamics F_ρ^s will reproduce the dynamical behavior of the driving module A. Although the persistence of the synchronized dynamics is guaranteed by condition (4), it is not at all clear that the synchronization manifold M itself is asymptotically stable with respect to the dynamics $\tilde{F}_\rho$. A periodic or chaotic orbit in M may be an attractor for the synchronized dynamics F_ρ^s but not for the dynamics $\tilde{F}_\rho$ of the coupled system. We therefore have to discuss stability aspects of the synchronized dynamics. As in [7] we will use the *synchronization exponents* λ_i^s and *conditional exponents* $\lambda_i^\perp$, $i = 1, \ldots, n$. They are derived from the linearizations $L^A(s(t))$ and $L^B(s(t))$ of corresponding module dynamics along synchronized orbits $s(t)$, i.e. we have

$$L_{ij}^{A}(s) := w_{ij}^{A} \cdot \sigma'(s_j) \, , \quad L_{ij}^{B}(s) := w_{ij}^{B} \cdot \sigma'(s_j) \, , \quad i, j = 1, 2 \ . \tag{8}$$

Synchronization exponents λ_i^s will be calculated from the eigenvalues of matrix L^A, and conditional exponents $\lambda_i^\perp$ from those of L^B. Synchronized chaotic dynamics will be characterized by a situation where at least one synchronization

exponent satisfies $\lambda^s > 0$. On the other hand, a positive conditional exponent indicates an unstable synchronization manifold M. Thus, if an unstable M contains a chaotic orbit the system naturally must have entered a *hyperchaotic* regime [8]; i.e. at least two Lyapunov exponents of the synchronized dynamics F^s_ρ are positive.

For a better characterization of attractors in coupled neuromodules the following definition is found useful [1]: A quasiperiodic or chaotic attractor is called *p-cyclic* if it has p connected components which are permuted cyclically by the map $\tilde{F}_\rho$. Every component of a p-cyclic attractor is an attractor of $\tilde{F}^p_\rho$.

3 Coupled 2-neuron modules

As a driving module we will chose in the following the chaotic 2-module [4] composed of an excitatory neuron coupled bi-directionally with an inhibitory neuron with self-connection. Its dynamics is given by a five parameter family of maps $f_\rho : \mathbf{R}^2 \to \mathbf{R}^2$ defined by

$$\begin{aligned} a_1(t+1) &:= \theta_1^A + w_{12}^A\,\sigma(a_2(t))\ , \\ a_2(t+1) &:= \theta_2^A + w_{21}^A\,\sigma(a_1(t)) + w_{22}^A\,\sigma(a_2(t))\ . \end{aligned} \tag{9}$$

This module has chaotic chaotic attractors for parameters around $\theta_1^A = 3$, $\theta_2^A = -2$, $-w_{12}^A = w_{21}^A = 6$, and $w_{22}^A = -16$. We will use this module to drive another 2-neuron module into complete synchronized states. The two configurations we will study are shown in figure 1a, b. The fist setup couples the inhibitory neurons of modules A and B in a uni-directional way, the second case will consider the coupling from the inhibitory neuron of A to the excitatory one of B.

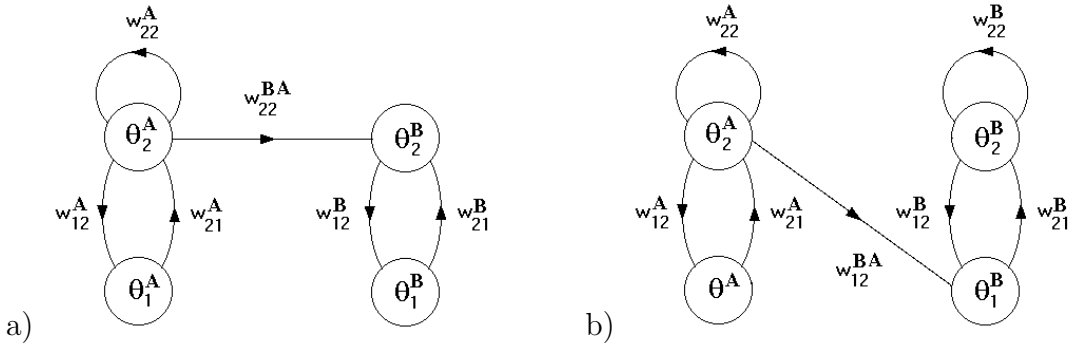

Figure 1: Two types of coupling modules in an uni-directional way: Neurons 1^A, 1^B are excitatory, neurons 2^A, 2^B are inhibitory.

3.1 Coupling inhibitory units

If we choose an uni-directional coupling $w_{22}^{BA} \neq 0$, then the driven module B must have parameters identical to that of A, with the exception that w_{22}^{B}, according to the synchronization condition (4, must satisfy $w_{22}^{B} = (w_{22}^{A} - w_{22}^{BA})$. We will study the extreme case where $w_{22}^{BA} = 0$; i.e. the isolated module B has no self-connections, and its dynamics has only fixed point or period-4 attractors [5].

Simulations reveal that stable synchronization of this setup is feasible. For demonstration we calculated the synchronization and conditional Lyapunov exponents λ_i^s and $\lambda_i^\perp$, $i = 1, 2$, respectively, for a bifurcation sequence of the synchronized dynamics shown in figure 3. The result is presented in figure 2, where only the largest exponents λ_1^s and $\lambda_1^\perp$ are drawn.

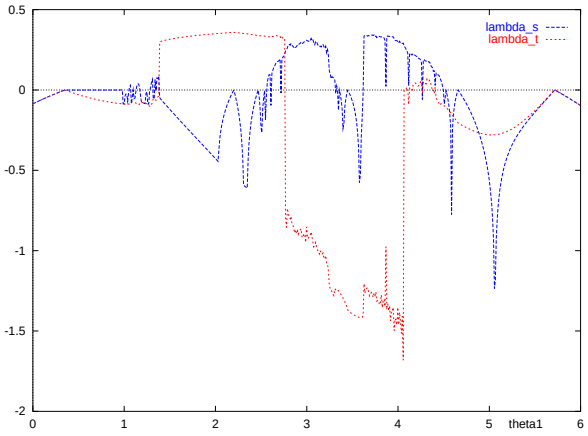

Figure 2: Largest synchronization and conditional exponents for fixed parameters $\theta_2 = -2$, $-w_{12} = w_{21} = 6$, $w_{22}^{A} = -16$, $w_{22}^{BA} = -16$, and varying θ_1.

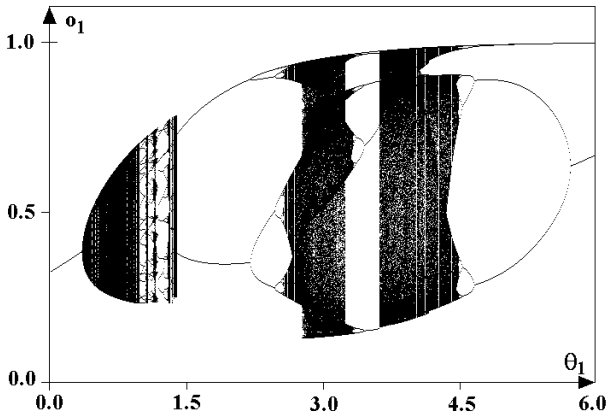

Figure 3: Bifurcation diagram of the synchronized dynamics for the same parameter values as in figure 2.

Synchronized dynamics starts with a fixed point attractor at $\theta_1 = 0$. Then there follows a bifurcation to quasiperiodic attractors, a small window with various bifurcation sequences to chaos, and after a larger period-2 interval, there is a (forward and backward) period-doubling route to chaos ending again in a period-2 attractor for $\theta_1 = 6$. From figure 2we read that there are θ_1-intervals, for which the conditional exponent $\lambda_1^{\perp}$ is positive; i.e. the corresponding synchronized dynamics on M is unstable. The underlying data file locates the larger interval as $(1.39, 2.76)$, and a smaller one at $(4.09, 4.37)$. In the last θ_1-interval we will find unstable synchronized chaos, as in the interval $(2.57, 2.76)$. Outside of these intervals we find synchronized fixed point, periodic, quasiperiodic, as well as synchronized chaotic attractors.

In fact, also co-existing attractors constrained to the stable synchronization manifold M can be observed. For $\theta_1 = 1.3$, for example, we find synchronous period-5, and period-14 attractors in addition to a synchronous chaotic attractor. In figures 5 to 6 some of the observed dynamical features are documented : Left figures show projections of attractors onto the (o_1^A, o_2^A)-phase space of the driving module A, the right hand figure projections onto the (o_1^A, o_1^B)-output space of the coupled system. Synchronized outputs will appear as states on the main diagonal in (o_1^A, o_1^B)-space. The parameters $\theta_2 = -2$, $-w_{12} = w_{21} = 6$, $w_{22}^A = w_{22}^{BA} = -16$ are fixed. Figure 4, for $\theta_1 = 3$, displays an example of an (presumable globally) stable synchronous attractor (right), driven by the chaotic attractor of module A (left). In figure 5, for $\theta_1 = 4.1$, the driving dynamics is a 2-cyclic chaotic attractor. Coupling w_{22}^{BA} results here in a 2-cyclic chaotic attractor, one part of which corresponds to synchronized units 1^A and 1^B and asynchronous units 2^A and 2^B, the other part is asynchronous on 1^A, 1^B and gives synchronized units 2^A and 2^B. This means, that at every second time step t the outputs satisfy $o_1^A(t) = o_1^B(t)$, $o_2^A(t) \neq o_2^B(t)$ and for $t+1$ synchronization is the other way round. Finally, in figure 6 a driving 2-cyclic chaotic attractor for $\theta_1 = 2.7$ produces, depending on initial conditions, a synchronous chaotic attractor co-existing with a 2-cyclic chaotic attractors. This second attractor has again an asynchronous part and a synchronous part (the shorter line in the upper right corner).

3.2 Coupling inhibitory and excitatory units

The same type of dynamical phenomena - synchronized periodic, quasiperiodic and chaotic attractors, and the co-existence of synchronous and asynchronous attractors - are also observed for other one-way coupling schemes satisfying the synchronization condition (4). For instance, one may couple two chaotic modules of the kind given by equations (9) by setting only $w_{12}^{BA} \neq 0$ as shown in figure 1b. Then the connection w_{12}^B must satisfy $w_{12}^B = w_{12}^A - w_{12}^{BA}$. In the following parameters are set to $\theta_2 = -2$, $w_{21} = 6$, $w_{22} = -16$, $w_{12}^A = -6$, $w_{12}^B = -3$ and $w_{12}^{BA} = -3$, and θ_1 varying. As isolated module, B inherits only period-2 attractors over the whole input interval $0 \leq \theta_1 \leq 6$.

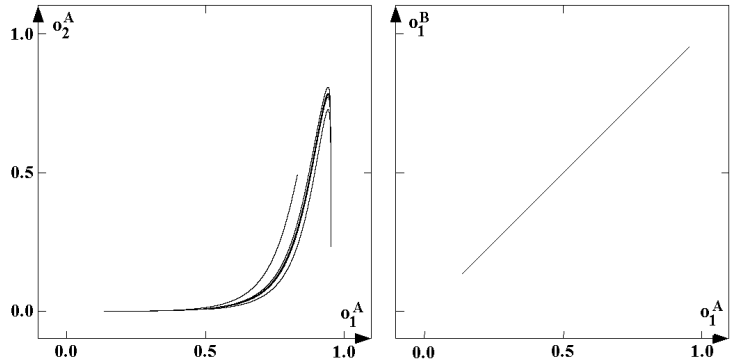

Figure 4: A synchronous chaotic attractor. Projections to module space (left) and to the output space of the coupled system (right). Parameters: $\theta_1 = 3$, $\theta_2 = -2$, $-w_{12} = w_{21} = 6$, $w_{22}^A = -16$, $w_{22}^{BA} = -16$.

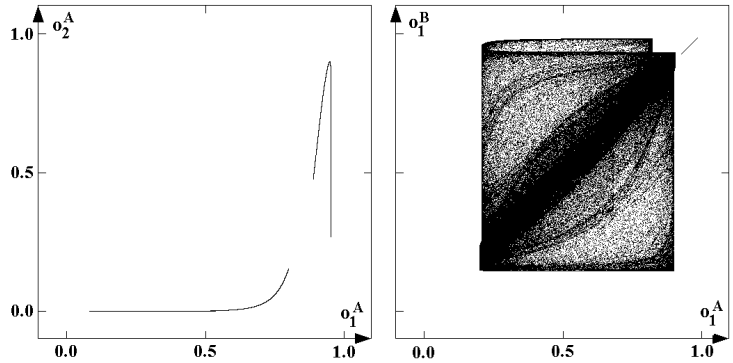

Figure 5: A driven 2-cyclic chaotic attractor with one part situated on the synchronization manifold M. Parameters as for figure 4 but with $\theta_1 = 4.1$.

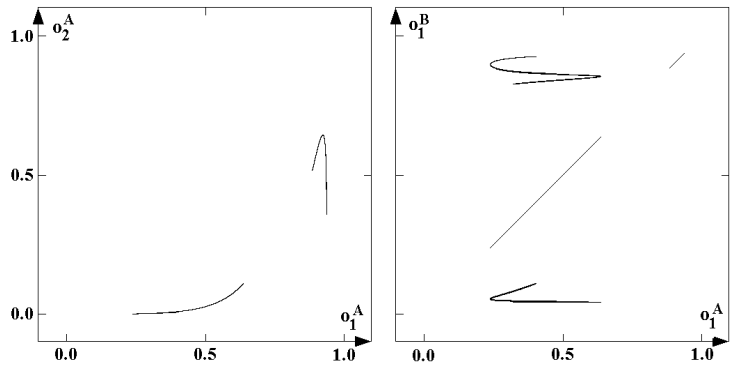

Figure 6: A synchronous chaotic attractor co-existing with an asynchronous 2-cyclic chaotic attractor. They are driven by a 2-cyclic chaotic attractor. Parameters as for figure 4 but with $\theta_1 = 2.7$

According to equation (7), the synchronized dynamics for identical inputs $\theta^A = \theta^B$ is the same as that of the above example, and as is displayed in figure 3. But the stability of the synchronous dynamics on M is quite different, as can be read by comparing the conditional Lyapunov exponents in figures 2 and 7.

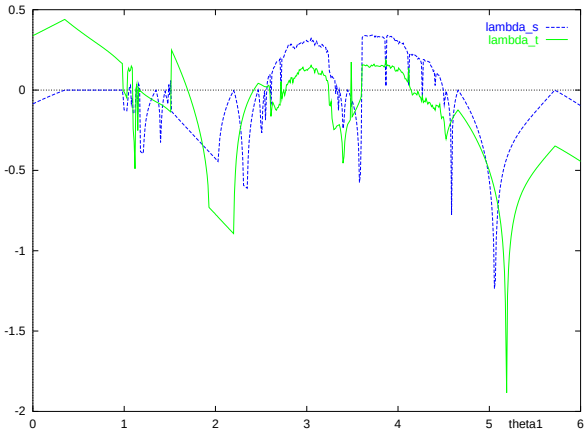

Figure 7: Largest synchronization and conditional exponents for fixed parameters $\theta_2 = -2$, $w_{21} = 6$, $w_{22} = -16$, $w_{12}^A = -6$, $w_{12}^B = -3$ and $w_{12}^{BA} = -3$, and varying θ_1.

For instance, there is no stable synchronization for small inputs $0 \leq \theta_1 \leq 1$. On the other hand, around $\theta_1 = 2$, there is a stable synchronization on a period-2 attractor, which coexists with an asynchronous one; where as for coupled inhibitory units we have unstable synchronization.

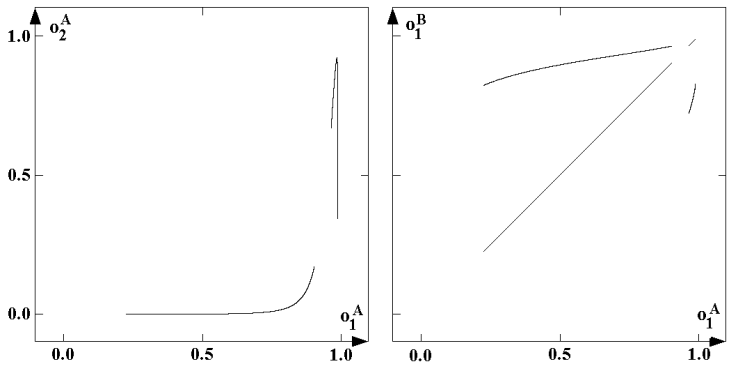

Figure 8: A driving 2-cyclic chaotic attractor (left) giving a synchronous 2-cyclic chaotic attractor and a co-existing asynchronous one (right). Projections to module space (left) and to the output space of the coupled system (right). Parameters: $\theta_1 = 4.3$, $\theta_2 = -2$, $w_{12}^A = -6$, $w_{12}^B = -3$, $w_{21} = 6$, $w_{22} = -16$, and $w_{12}^{BA} = -3$.

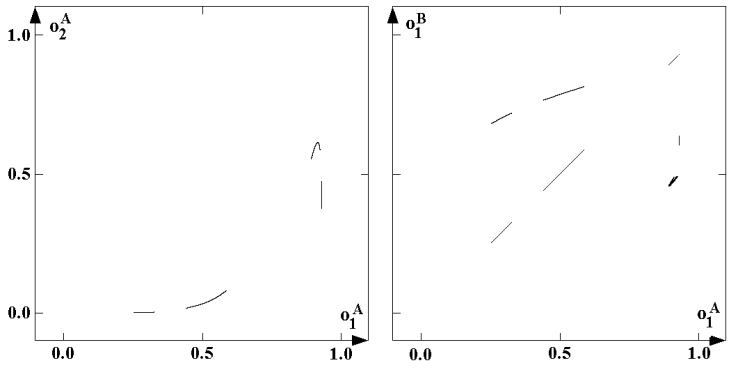

Figure 9: A 4-cyclic chaotic attractor co-existing with an asynchronous one. Parameters as for figure 8 but with $\theta_1 = 2.6$.

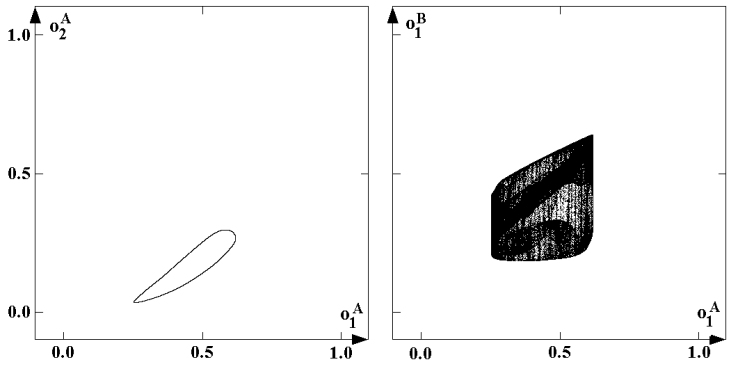

Figure 10: An asynchronous chaotic attractor resulting from a driving quasiperiodic attractor. Parameters as for figure 8 but with $\theta_1 = 0.7$

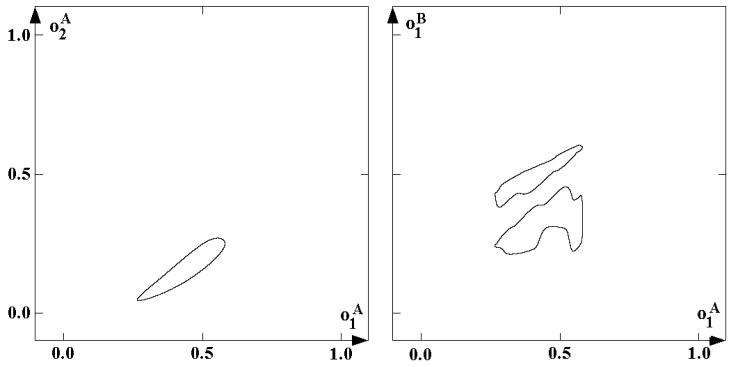

Figure 11: An asynchronous 2-cyclic quasiperiodic attractor driven by a quasiperiodic attractor. Parameters as for figure 4 but with $\theta_1 = 0.6$

4 Conclusions

It has been shown that in a system composed of simple neuromodules synchronization of non-trivial discrete-time dynamics is feasible already by a one-way coupling of modules. For a synchronous dynamics to exist, the sum of external stationary inputs and bias terms of corresponding module units has to be identical. Depending on module parameters, the synchronized orbits can be locally or globally stable, or unstable. Remarkable seems to be the existence of a strange type of chaotic attractor depicted in figure 5; it shows a 2-cyclic chaotic attractor with one part consisting of synchronized states and the other part being hyperchaotic. This means that one part is a synchronous chaotic attractor of $\tilde{F}_\rho^2$ the other is a hyperchaotic attractor of $\tilde{F}_\rho^2$.

Simulations, not only for the example presented here, convinced us that in general there are larger parameter domains for which stable synchronized chaos will exist. Noteworthy is also the fact that synchronous dynamics often co-exists with different kinds of asynchronous dynamics. Thus, (locally) stable synchronization depends on initial conditions, that is, on the "history" of the coupled system.

Furthermore, a synchronized mode often persists even if external inputs are varying slowly. Thus, synchronization of coupled modules is really a sign for time-varying (identical) input signals with amplitudes having a *fixed ratio* (recall, that the inputs may correspond to the weighted outputs of other neurons in a larger system). De-synchronizing the coupled modules is of course easily done: Either by diverging inputs or by steering the coupled modular system into parameter domains for unstable synchronization.

The general synchronization condition (3) allows also a bi-directional coupling of neurons. Analysis and result from computer simulations for special kinds of recurrently coupled neuromodules will be presented elsewhere [6].

References

[1] Abraham, R. H., Gardini, L. and Mira, C. (1997), *Chaos in Discrete Dynamical Systems*, Springer-Verlag, New York.

[2] Kapitaniak, T. (1996). *Controlling Chaos - Theoretical and Practical Methods in Non-linear Dynamics.* San Diego: Academic Press.

[3] De Sousa Viera, M., Lichtenberg, A. J. and Liebermann, M.A. (1992) Synchronization of regular and chaotic systems, *Phys. Rev. A*, **46**, 7359–7362.

[4] Pasemann, F. (1995). Neuromodules: A dynamical systems approach to brain modelling. In H. Herrmann, E. Pöppel, D. Wolf (eds.), *Supercomputing*

in Brain Research - From Tomography to Neural Networks, (pp. 331–347). Singapore: World Scientific.

[5] Pasemann, F. (1995), Characteristics of periodic attractors in neural ring networks, *Neural Networks*, **8**, 421-429.

[6] Pasemann, F. (1999), Synchronous and asynchronous chaos in coupled neuromodules, submitted for publication.

[7] Pecora, L. M. and Carroll, T. L. (1990), Synchronization in chaotic systems, *Phys. Rev. Lett.*, **64**, 821–823.

[8] Rössler, O. (1979) An equation for hyperchaos. *Phys. Lett. A*, **71**, 155-157.

[9] Singer, W. (1994) Time as coding space in neocortical processing. In Buzsáki, G.; Llinás, R.; Singer, W.; Berthoz, A. and Christen, Y. (eds.) *Temporal Coding in the Brain*. Springer, Berlin. pp. 51-80.